Optical properties of poly-HCN and their astronomical applications

BISHUN N. KHARE,[1] CARL SAGAN, AND W. REID THOMPSON
Laboratory for Planetary Studies, Cornell University, Ithaca, NY 14853, U.S.A.
AND
EDWARD T. ARAKAWA, CAROLINE MEISSE, AND PAGE S. TUMINELLO[2]
Health and Safety Research Division, Oak Ridge National Laboratory, Oak Ridge, TN 37831, U.S.A.
Received July 27, 1993
This paper is dedicated to Professor John C. Polanyi on the occasion of his 65th birthday

BISHUN N. KHARE, CARL SAGAN, W. REID THOMPSON, EDWARD T. ARAKAWA, CAROLINE MEISSE, and PAGE S. TUMINELLO. Can. J. Chem. **72**, 678 (1994).

Matthews (1992) has proposed that HCN "polymer" is ubiquitous in the solar system. We apply vacuum deposition and spectroscopic techniques previously used on synthetic organic heteropolymers (tholins), kerogens, and meteoritic organic residues to the measurement of the optical constants of poly-HCN in the wavelength range 0.05–40 μm. These measurements allow quantitative comparison with spectrophotometry of organic-rich bodies in the outer solar system. In a specific test of Matthews' hypothesis, poly-HCN fails to match the optical constants of the haze of the Saturnian moon, Titan, in the visible and near-infrared, derived from astronomical observations and standard models of the Titan atmosphere. In contrast, a tholin produced from a simulated Titan atmosphere matches within the probable errors. Poly-HCN is much more N-rich than Titan tholin.

BISHUN N. KHARE, CARL SAGAN, W. REID THOMPSON, EDWARD T. ARAKAWA, CAROLINE MEISSE et PAGE S. TUMINELLO. Can. J. Chem. **72**, 678 (1994).

Matthews (1992) a suggéré que le HCN à l'état de polymère est omniprésent dans le système solaire. Dans ce travail, on applique des techniques de déposition sous vide et spectroscopiques utilisées antérieurement sur des hétéropolymères organiques de synthèse (« tholines »), des kérogènes et des résidus organiques météoritiques pour mesurer les constantes optiques du poly-HCN aux longueurs d'onde allant de 0,05 à 40 μm. Ces mesures permettent d'établir une comparaison quantitative avec la spectrophotométrie de corps riches en produits organiques dans le système solaire externe. Dans le cas spécifique de la vérification de l'hypothèse de Matthews, le poly-HCN ne concorde pas avec les constantes optiques de la brume de la lune de Saturne, Titan, dans le visible et le proche infrarouge qui ont été obtenues à partir d'observations astronomiques et de modèles standard de l'atmosphère de Titan. Par ailleurs, une tholine produite dans un atmosphère de Titan simulé concorde aux erreurs probables. Le poly-HCN est beaucoup plus riche en N que la tholine de Titan.
[Traduit par la rédaction]

1. Introduction

In a long series of papers, Clifford Matthews has argued that "polymeric" HCN may be readily formed in the solar system and may account for the dark surface coatings seen on many objects in the outer solar system. Specifically, claims are made for the dark involatile surface of the nucleus of Comet Halley, D-class asteriods, the rings of Uranus, the dark hemisphere of Iapetus, the orange-brown clouds of Jupiter and Saturn, and the haze of Titan (1–3).

Laboratory experiments have demonstrated that complex organic solids are readily formed by the action of UV light and (or) charged particles on atmospheres and icy surfaces containing simple carbon-bearing molecules. These heteropolymers are often generated by the participation of many chemical species, and mechanisms by which gas-phase species participate in forming the chemical structure of the solid have been proposed. Under more limited conditions, polymers may form from nearly pure starting materials — for example, UV light catalyzes the formation of "polyacetylenes" (polyethyne) in planetary atmospheres (4), and UV acting on solid ethyne in outer planet condensation hazes also produces polymeric residues.

Another widely discussed candidate for polymerization is HCN. While HCN is more often just one of many participating species in polymer formation (e.g., in the radiation chemistry of N_2–CH_4 atmospheres), "pure" HCN polymers are possible in principle. Whatever its chemical origin, the -C≡N (nitrile) group is important in organic residues in several types of solar system bodies: the 2.2 μm C≡N overtone band has been tentatively identified in the dust of "new" comets, on D-type asteroids, in the Uranian rings, and on the dark side of Iapetus (5). Matthews (6) claims that the polymerization of hydrogen cyanide is a universal process; CH_4 and NH_3 are simple cosmically abundant molecules that easily produce (7) HCN on irradiation with charged particles or UV photons; also, HCN is known to polymerize (8) in the condensed state or when irradiated as a gas, to "poly-HCN". The argument for "poly-HCN" rests on its alleged ease of formation and its dark color. No measurements of its optical constants have been made heretofore; no detailed comparison of laboratory and astronomical spectra has shown a best fit for "poly-HCN"; and no radiative transfer models have been used to compare laboratory optical constants of "poly-HCN" with the spectra of solar system bodies.

Generally, organic heteropolymers produced in astronomical environments where N atoms are available contain some nitrile component. Khare and Sagan (9) produced a brown organic solid by long-wavelength ultraviolet irradiation of abundant gases in reducing planetary atmospheres; the solid exhibits a 4.5 μm C≡N nitrile or isocyanide fundamental band. We proposed (9) that a heteropolymer containing nitriles and polynitriles may be a common constituent of aerosols in the outer solar system, and later coined the name tholin (10) for such complex materials. The 4.5 μm band was also found in tholin

[1]Author to whom correspondence may be addressed.
[2]Also at University of Tennessee, Knoxville, TN 37996, U.S.A.

made from equimolar amounts of CH_4 and NH_3 with 2.5% water vapor (11), and in Titan tholin (12) made from 90% N_2 and 10% CH_4.

In the identification, by Cruikshank et al., (5) of the 2.2 μm first overtone band of the C≡N fundamental in reflection spectra of several bodies throughout the outer solar system, the fit to tholins was at least as good as the fit to "poly-HCN". The two are far from being the same materials. At the very least, we can say that the 2.2 μm feature is not diagnostic of "poly-HCN". However, while we believe the C≡N bond in these materials usually arises from heteropolymers in whose formation HCN played at most only a part, pure "poly-HCN" provides an interesting end member of this class of organic solids.

Poly-HCN (henceforth, we drop the quotation marks) can be categorized (13) into three major forms: (*a*) true polymeric $(HCN)_n$, the repetition of the same monomeric unit *n* times; (*b*) HCN heteropolymer or oligomer (not polymer), which has the same rough abundance of organic functional groups producing roughly the same IR spectrum, but is not repetitive, especially in its hydrocarbon and other side chains; and (*c*) HCN aqueous solution polymer or oligomer, which contains oxygenated side chains and other components. These three different forms of poly-HCN need not have the same IR spectrum; e.g., form *c* does not exhibit the 4.5 μm C≡N absorption, or its corresponding 2.2 μm overtone. While HCN is an important minor species in some astronomical environments, it is hard to imagine atmospheres or ices in the solar system or beyond made of pure HCN, free of other components, and producing pure poly-HCN.

Laboratory experiments, done at Cornell University (14–16) and elsewhere, show that the gas- and solid-phase product molecules are diverse even in simulation experiments starting with only a few major precursor gases. We have found that tholin synthesized from a crude simulation of Jupiter is not pure poly-HCN but is a heteropolymer with a variety of moieties (13). The same conclusion is also drawn from the pyrolytic GC–MS results on this tholin as well as on Titan tholin (14, 15, 17); hundreds of pyrolytic products were detected in both tholins. But a diagnostic test is the comparison of laboratory optical constants of poly-HCN with optical constants derived from astronomical and spacecraft observations.

We previously (18, 19) applied the technique of thermal evaporation and successfully determined the optical constants of kerogen, the organic residue obtained from the Murchison carbonaceous chondrite, and ice tholin (made from charged particle irradiation of $C_2H_6/H_2O \sim 1{:}6$ at 77 K). Here we present results of measurements of the optical constants of poly-HCN in the form of thermally evaporated thin films.

Lunin et al. (20) have studied the properties of thin films of polyparacyanogen that, like poly-HCN, contains C≡N in its structure. They prepared a thin film by electron-beam evaporation in vacuum, a technique sometimes substituted for thermal evaporation in vacuum. They found that the preparation of thin films is very dependent on the structure of the original polymer. On the basis of the preservation of elemental (C, H, N) ratios and agreement of IR spectra of the original polymers and films, they conclude that electron-beam spray coating in vacuum leads to splitting of the macromolecules into low-molecular-weight fragments that completely preserve the chemical structure of the original polymer. These fragments, on deposition on the substrate, recombine to form macromolecules. Our experience with the vacuum evaporation technique applied to other organic residues indicates a similar preservation of the chemical character of the original material (18, 19).

2. Production of poly-HCN

2.1. Synthesis of HCN and poly-HCN

Hydrogen cyanide is readily produced by the action of electric discharges, high temperatures, or ionizing radiation upon a variety of reducing or nonoxidizing atmospheres. The yields are particularly high if electric discharges are applied. The type of atmosphere used for the source of H, C, and N atoms to produce HCN seems relatively unimportant until higher oxidation states are reached. Miller (21) produced HCN along with CO, CO_2, and N_2 from a mixture of CH_4, NH_3, H_2O, and H_2 after coronal discharge. Sagan and Miller (22), in an experiment crudely simulating the deep atmosphere of Jupiter, found HCN, CH_3CN, C_2H_2, C_2H_4, and C_2H_6 in a coronal discharge through a gas mixture containing H_2, CH_4, and NH_3, with H_2 in excess. Many subsequent experiments in neutral to reducing C- and N-containing gas mixtures also found HCN to be a major product. Cyanogen is routinely found in sunspots and in the photospheres of cool stars.

One of the common methods for preparing anhydrous hydrogen cyanide in the laboratory is by the action of sulfuric acid on sodium cyanide, potassium cyanide, or potassium ferrocyanide (23); for example,

$$[1] \qquad NaCN + H_2SO_4 \rightarrow HCN + NaHSO_4$$

In the Andrussow process, the major commerical method (24) for producing HCN gas, the reaction takes place between NH_3, CH_4, and air over a platinum catalyst at 1100°C:

$$[2] \qquad CH_4 + NH_3 + 1.5O_2 \rightarrow HCN + 3H_2O$$

Poly-HCN employed in our study was obtained from E.I. du Pont de Nemours & Co., Inc. Its infrared spectrum indicates that it is probably composed of a mixture of all three types of poly-HCN (13). Its IR spectrum is nearly identical to that of poly-HCN prepared by Matthews (see ref. 5).

Poly-HCN formation normally occurs in aqueous solution. It can also occur in anhydrous solvents, but requires a compound capable of creating CN^- ions in the solvent. Polymerization occurs readily when both CN^- and HCN are major components in solution, specifically, when $4.0 < pH < 10.5$. The rate of polymerization and the form of the final polymer will depend on the interactions with other species in solution. HCN does not polymerize in the vapor phase.

We obtained poly-HCN samples from two places in the du Pont manufacturing system. One sample came from piping immediately after the HCN production reactors. The products in reaction [2] are cooled to very near the dew point to remove water produced in the reaction. There are places in the piping where the gases are cooled locally to below the dew point and these aqueous droplets absorb some HCN and unreacted NH_3, which brings the pH into the polymerization range.

Another sample came from the purification train. Here HCN polymerizes from HCN in water with no additional solutes. The solutions are normally stabilized to pH <2 with an acid, but if HCN condenses in a spot where there is no acid, it will begin to polymerize and seed further polymerization. We used this poly-HCN sample collected from the walls of the purification line for optical constants measurements.

Völker (25, 26) proposes that poly-HCN is formed via imi-

TABLE 1. Elemental composition (weight percent)

Elements	Poly-HCN synthesized in water (26)	Anhydrous poly-HCN made in organic solvent (26)	du Pont poly-HCN (<0.03% sulfur impurity) employed in making film (this work)	Tholin from plasma discharge through 9:1 N_2/CH_4 mixture at 0.2 mbar pressure (11, 12)	Tholin reactant composition (12)
C	41.4	45	30.7	47.7	4.48
H	4.0	4.0	4.1	6.4	1.50
N	43.2	51.3	46.7	29.3	94.02
O	11.4		18.5	16.6	

noacetonitrile, which is a dimer of hydrogen cyanide and is considered to be formed by reaction between HCN and CNH according to a scheme known for the addition of isonitriles to nitriles:

[3] $HCN + CNH \rightarrow H-C(=N-H)-C\equiv N$

A recent study of HCN dimers was made by Evans et al. (27, 28). Some controversy over the structure of dimeric HCN is summarized by Ferris and Hagan (29). A detailed study of the mechanism of HCN polymerization has been given by Sanchez et al. (30), Ferris et al. (31), Ferris and Edelson (32), and Ferris (33).

2.2. *Properties of HCN and poly-HCN*

While HCN is a colorless, poisonous, low-viscosity liquid said to have an odor characteristic of bitter almonds, poly-HCN is a brown-black solid having hardly any odor, although a freshly prepared poly-HCN has a slight odor of the monomer and, occasionally, of ammonia (26). Poly-HCN is not known to have any toxic effects. Details on the synthesis and structure of poly-HCN were given recently by Matthews and Ludicky (34) and earlier by Völker (26).

HCN has a melting point of −13.24°C, a boiling point of 25.70°C, and a density 0.7150 g cm^{-3} at 0°C. It can polymerize violently in the presence of heat, alkaline materials, or moisture. Once initiated, polymerization becomes uncontrollable since the reaction is autocatalytic, producing heat and alkalinity (NH_3). Confined polymerization can cause a violent explosion.[3] This is part of the appeal of the proposal that cometary outbursts are due to HCN polymerization (35).

The density of poly-HCN was measured by determining the weight and volume of a 13 mm pellet of poly-HCN prepared by compressing du Pont poly-HCN powder at 1700 atmospheres. A density of 1.49 g cm^{-3} was obtained; this is a lower limit due to residual void space inside the pellet. The density of our evaporated films, prepared subsequently, was measured using the float and sink method (employing a series of varying density solutions made from CCl_4 and CH_3OH). This method yielded a value of 1.54 ± 0.005 g cm^{-3}. The density of unpressed fluffy du Pont poly-HCN powder, determined by helium pycnometry, gave a value of 1.620 ± 0.004 g cm^{-3}. This technique avoids error caused by void volume and should be taken as the best value for the density of du Pont poly-HCN.

The average value of the atomic composition of du Pont poly-HCN determined by Schwarzkopf Microanalytical Laboratory and Galbraith Laboratories, Inc. (after correcting for oxygen and hydrogen due to exposure of poly-HCN to 0.034% SO_2 and 0.026% H_2SO_4 used as a stabilizer for HCN gas in the du Pont manufacturing plant) is given in Table 1. The balance of the remaining large amount of oxygen in this kind of sample probably occurs from the interaction of the poly-HCN with H_2O during formation from the product stream. No correction for oxygen or hydrogen due to exposure of poly-HCN to water (or subsequent exposure to air) is made.

The sulfur, oxygen, and incremental hydrogen impurities are due to exposure of poly-HCN to sulfur compounds and water in the plant and, perhaps, to the air during storage of the poly-HCN. These impurities do not affect the measurement of the optical constants, since infrared spectra of the evaporated and redeposited film of poly-HCN at 800 K agree with those of the anhydrous poly-HCN of Völker (26) and Cruikshank et al. (5).[4] Table 1 also includes; for comparison, the average elemental composition of Titan tholins determined by Schwarzkopf and Galbraith. It clearly shows that poly-HCN and Titan tholin have very different elemental compositions, as is also reflected in their optical constants (see below).

2.3. *Comparison of the infrared spectra of poly-HCN from several sources*

Völker (26) has shown that poly-HCN synthesized in water has elemental composition 41.4% C, 4.0% H, and 43.2% N. The remaining ~11% he attributes to O atoms without indicating any specific position for the oxygen atoms in the proposed structure of the poly-HCN (Fig. 1(*a*)). No IR band corresponding to the C≡N stretching vibration at 4.5 μm is found in the transmission spectrum. Anhydrous poly-HCN (Fig. 1(*b*)) made in organic solvents such as chloroform has elemental composition 45% C, 4.0% H, and 51.3% N and exhibits a strong C≡N band at 4.5 μm. The presence and absence of this feature results from different structures of the monomer units as shown in Figs. 1(*a*) and (*b*). Völker (26) finds that the oxygen does not react with the polymer, but the presence of water vapor in moist air causes oxygen to be incorporated into the polymer. Cruikshank et al. (5) report that anhydrous poly-HCN (Fig. 1(*b*)) shows a diminution of the 4.5 μm feature with time, on treating with water at room temperature until its complete disappearance after 6 months.

Figure 2 shows the transmission and reflectance spectra of poly-HCN from du Pont Co. thermally evaporated and redeposited in our laboratory, compared with poly-HCN from several sources. "Electropolymeric" HCN (36) prepared by

[3]du Pont Material Safety Data Sheet H-12264-1. du Pont Co., Chemicals and Pigments Department, Chestnut Run Plaza, P.O. Box 80709, Wilmington, Del. (1989).

[4]D.P. Cruikshank et al. Private communication (1993).

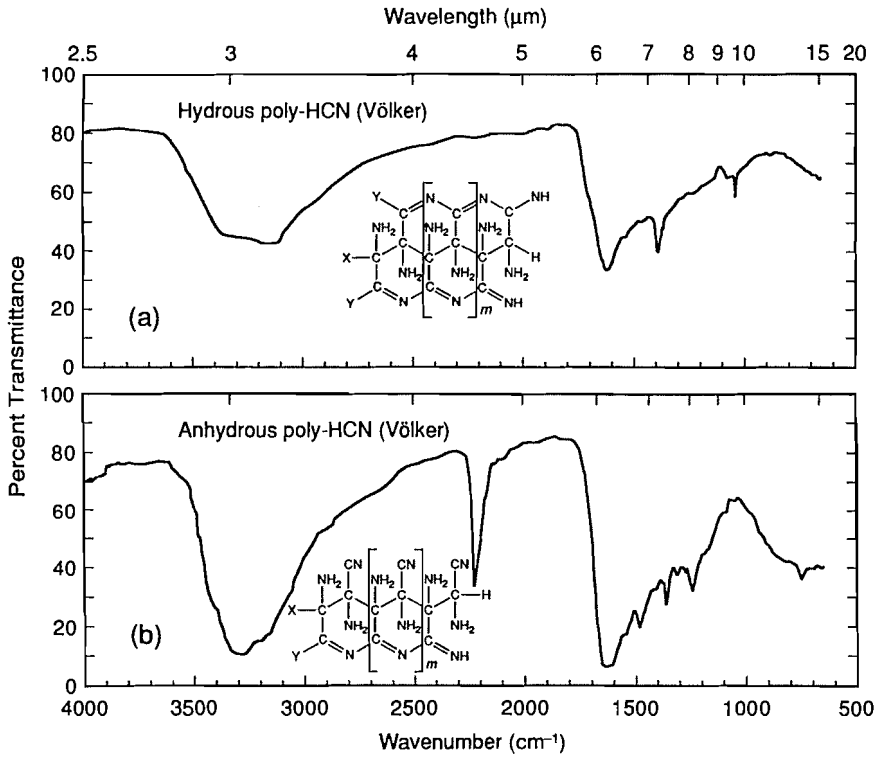

FIG. 1. Infrared spectra of poly-HCN (*a*) synthesized in water and (*b*) synthesized in organic solvents such as chloroform. Both spectra are taken from Völker (26). Note the similarity of (*b*) with Fig. 2(*b*) below, allowing for the lower resolution here.

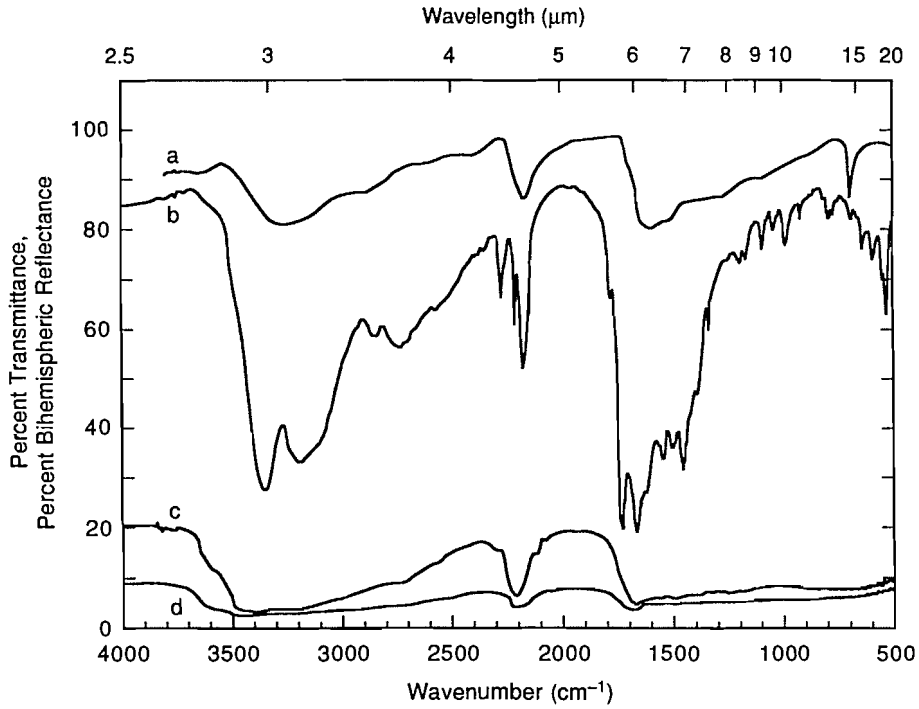

FIG. 2. Comparison of the infrared transmission spectra of (*a*) electropolymeric-HCN (arbitrary units) (36) with (*b*) thermally evaporated and redeposited poly-HCN from du Pont de Nemours under high vacuum in the present work, (*c*) bihemispheric reflectance spectrum of anhydrous poly-HCN (5, footnote 4), and (*d*) bihemispheric reflectance spectrum of hydrous poly-HCN (5, footnote 4).

0.5 mA arc discharge through HCN shows weak IR absorptions. The reflection spectrum of anhydrous poly-HCN is from a sample prepared by Matthews and Ludicky in which liquid HCN with a catalytic trace of triethylamine was allowed to stand at room temperature for 30 days. Ammonia can also be used in place of triethylamine as a catalyst (7, 8). The initially colorless liquid becomes a yellow-orange-brown sludge, ending as a dark brown, almost black, powder (5). The hydrated poly-HCN is obtained by stirring this powder in cold water for 3 days and drying to yield a black solid material. The

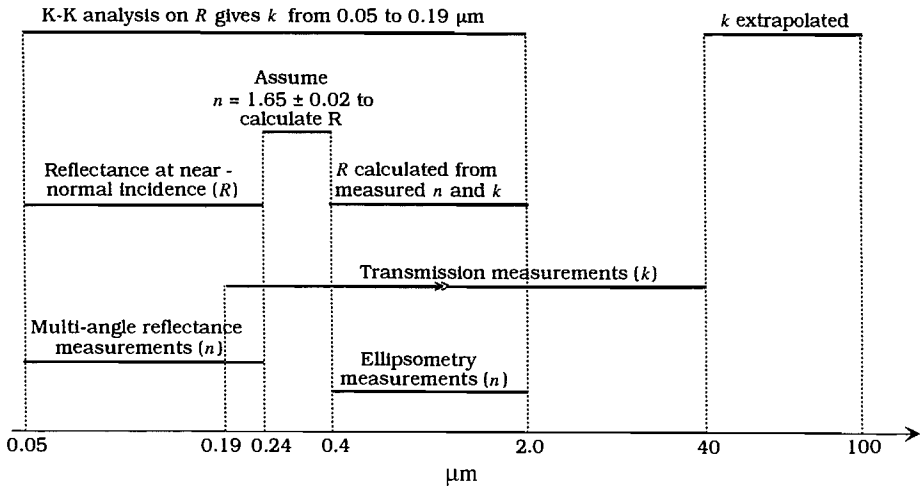

FIG. 3. Techniques employed in the measurement of the optical constants of a film prepared by thermal evaporation of poly-HCN and redeposition under high vacuum. The assumed value of n derives from ellipsometry.

reflection spectra of both anhydrous and hydrous poly-HCN obtained by Cruikshank et al.[4] are also reproduced here (Fig. 2). The comparison is only qualitative. Our vacuum-evaporated film exhibits all the major bands corresponding to functional groups present in the unheated poly-HCN from other sources, but the relative strength of the bands varies considerably. It is not expected that poly-HCN prepared under different conditions will produce identical infrared spectra (13).

3. Experimental

As discussed earlier (18, 19) in our continuing studies of the optical properties of organic residues, it is difficult to measure the imaginary part, k, of the complex refractive index by transmission measurements of solid materials that are in powdery form, since pulverized samples cause severe multiple scattering of the incident light. It is necessary instead to prepare optical quality films, particularly for the transmission measurements in the UV and visible where scattering is the greatest.

3.1. Thin film preparation

We prepared optical quality thin films of poly-HCN by thermal evaporation under high vacuum as described elsewhere (19). It was not possible to make suitable films thicker than $t = 1.5$ μm since thick films contained foggy areas. We therefore produced films of various thicknesses ranging from 0.05 to 1.5 μm. The exact thickness of the films is checked only after the spectral measurements are completed. A Sloan Angstrometer (model M-100) was used to measure the thickness of the thinner films. For $t \simeq 0.75$ μm, we measured the thickness from the interference pattern produced by light reflected from the front and back surfaces of the film in the wavelength range 0.4–2.5 μm, assuming an index of refraction $n = 1.65 \pm 0.02$ for this region. This value of n was determined previously by an independent ellipsometric measurement on a pressed pellet of poly-HCN.

Evaporation took place at a temperature of 800 ± 100 K at 10^{-5}–10^{-6} Torr (1 Torr = 133.3 Pa). The color of the molybdenum crucible at which the poly-HCN began to evaporate was used to determine the temperature. Evaporated poly-HCN was condensed onto optical quality CsI and CaF_2 substrates transparent from 0.3 to 50 μm and from 0.13 to 9 μm, respectively, and kept at room temperature. The thin films were colorless initially, turning yellowish with increasing thickness. By weighing the molybdenum crucible before and after evaporation, we determined that ~80% of the poly-HCN was evaporated.

3.2. Spectroscopic measurements

The infrared spectrum from 2.5 to 40 μm of unheated poly-HCN was obtained by measuring the transmission through a compressed pellet in a CsI matrix using a Mattson Galaxy 6020 FTIR spectrometer at 1 cm^{-1} resolution. The transmission spectrum from 2.5 to 40 μm of vacuum-evaporated films of poly-HCN on CsI substrates was obtained using a Perkin–Elmer model 983 spectrometer, also at 1 cm^{-1} resolution. Shimadzu UV250 and Cary 14 spectrophotometers were used in the ranges 0.19–0.9 μm and 0.4–2.5 μm, respectively. A Seya–Namioka monochromator was used from 0.13 to 0.4 μm for transmission measurements and from 0.13 to 0.24 μm for reflectance measurements. A McPherson model 247 grazing incidence monochromator enabled us to extend the reflectance measurements down to 0.05 μm.

Figure 3 summarizes the techniques used in the determination of the optical constants n and k, as discussed in detail elsewhere (12, 18, 19). Figure 4(*a*) shows the spectrum of unheated poly-HCN in a CsI matrix using a technique described by Khare and Sagan (37), and Fig. 4(*b*) shows the spectrum of a vacuum-evaporated and redeposited film of poly-HCN. We find that the du Pont poly-HCN (Fig. 4(*a*)) is not as hydrous as the hydrous poly-HCN of Völker (26) (Fig. 4(*d*)). The features in unheated du Pont poly-HCN better resemble those of the anhydrous poly-HCN (Fig. 4(*c*)) of Völker (26). This is reasonable since the du Pont poly-HCN is a mixture of both hydrous and anhydrous polymers. The infrared spectrum of our thermally evaporated film (Fig. 4(*b*)) is close to that of anhydrous poly-HCN (Figs. 1(*b*), 4(*c*)). The thermal evaporation technique has the advantage of removing adsorbed water and producing films exhibiting the strong band at 4.5 μm (2222 cm^{-1}) characteristic of C≡N as seen in the spectrum of anhydrous poly-HCN.

Films prepared by thermal evaporation under high vacuum (Fig. 4(*b*)) were used in the present investigation for the determination of the optical constants. These films are suspected to be more anhydrous than the anhydrous poly-HCN of Völker (26) as seen in the increase in the strength and multiplicity of the C≡N band at 4.5 μm if the decrease in the strength and multiplicity of the C≡N band is directly related to the degree of hydrolysis of poly-HCN. Table 2 lists all the bands found in our thermally evaporated films of poly-HCN. The infrared spectrum of a complex organic solid such as poly-HCN shows absorption bands that are due to well-known chemical functional groups. Possible assignments of some of the bands based on Bellamy (38), Szymanski (39), Pasto and Johnson (40), and Colthup (41) are presented in Table 2. These assignments are tentative and could change when the structure of this poly-HCN is better determined. The appearance of the C≡N spectral feature, as well as its strength and position, is known to vary from sample to sample. Our evaporated poly-HCN, being a mixture of all three types of poly-HCN and free from water, produces four distinct peaks, varying in intensity and wavelength, near 4.5 μm.

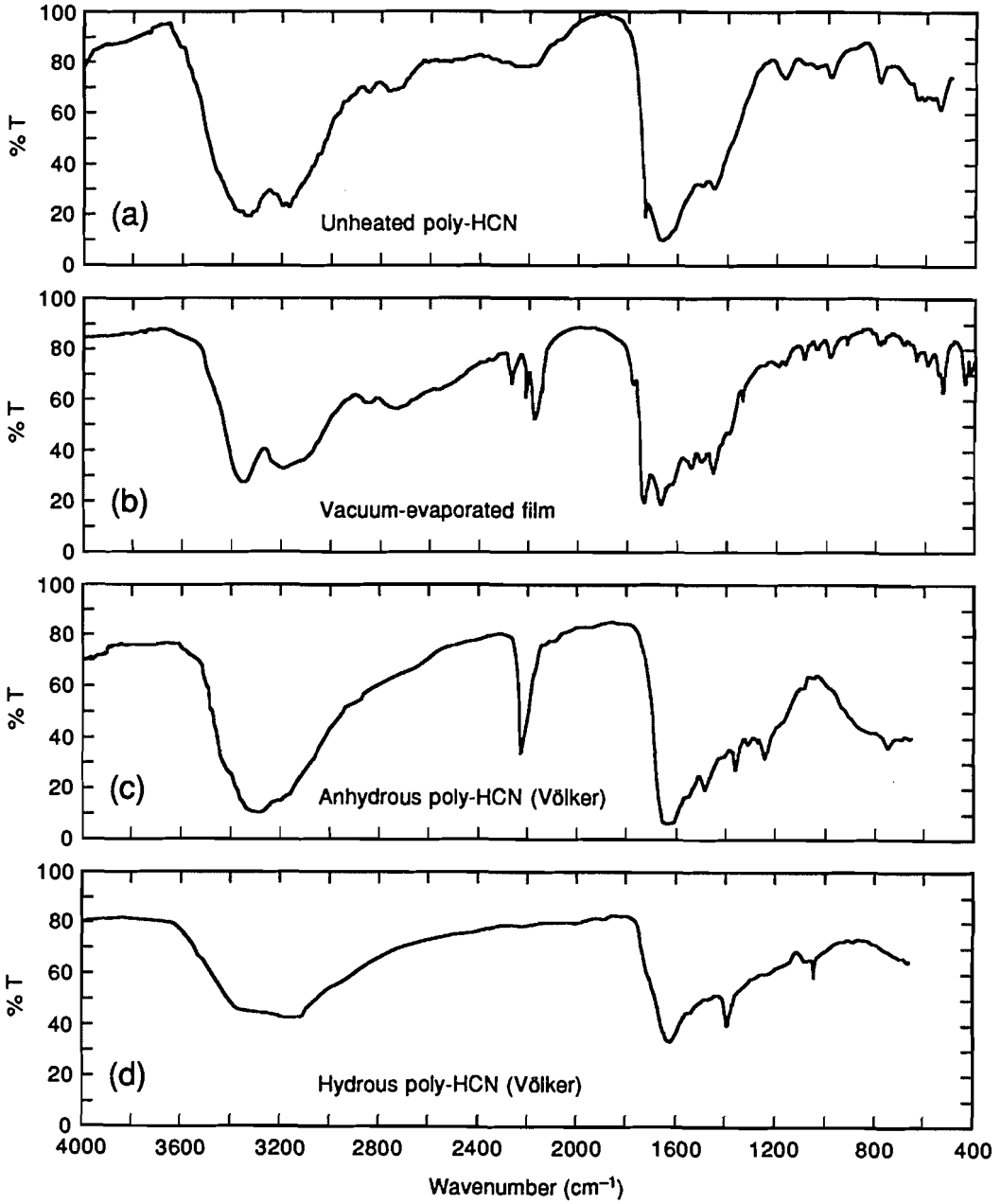

FIG. 4. Infrared spectra of poly-HCN (*a*) unheated in CsI matrix, (*b*) vacuum evaporated and redeposited at 800 ± 100 K on a CsI substrate, compared with (*c*) anhydrous poly-HCN made in organic solvents such as chloroform (26), and (*d*) hydrous poly-HCN made in water (26).

4. Optical constants

4.1. Direct measurements of the real part of the refractive index n

We measure n directly on films of evaporated poly-HCN using ellipsometry from 0.4 to 2 μm and multi-angle reflectance from 0.05 to 0.24 μm, as previously described (12). We also carried out ellipsometric measurements on solid pressed pellets made from unheated poly-HCN.

4.2. Direct measurement of the imaginary part of the refractive index k

The transmittance T of a thin film with thickness t on a thick substrate is given by Khare et al. (12) as

$$[4] \qquad T = T_s \frac{(1-R)}{(1-R_0)^2} \exp(-4\pi kt/\lambda)$$

where T_s = transmission of the bare substrate, R = normal-incidence reflectance of the film–substrate system, $R_0 = [(n_s - 1)/(n_s + 1)]^2$ is the normal-incidence reflectance at the substrate–air interface, and n_s is the real part of the refractive index of the substrate.

By considering R as independent of t, we determined k from the slope of the straight line drawn by plotting $\ln(T_s/T)$ against t. The advantage of this method is that we did not need to know n for either the substrate or the film. k was determined in this way from 0.19 to 40 μm.

4.3. Kramers–Krönig (K–K) analysis of k

For the wavelength range 0.05–0.19 μm, where it was not possible to measure k directly due to low film transmission and lack of suitable substrates, we determined k from reflectance measurements using the Kramers–Krönig relation given by dis-

TABLE 2. Assignment[a] of absorption features in the infrared spectra of anhydrous thermally evaporated poly-HCN under high vacuum

Frequency (v) cm^{-1}	Wavelength (λ)(μm)	intensity[b]	Vibrational classification	Functional groups
3380	2.99	vs	Hydrogen bonded N—H stretching	Aromatic
3185	3.14	vs	C—H stretching or N—H stretching	Aromatic
2850	3.51	m	$—CH_2$	
2730	3.66	m	—[c]	
2565	3.90	m	—[c]	
2265	4.42	m	C≡N stretching	Aromatic
2208	4.53	m		
2170	4.61	m		
2150 sh	4.65 sh	m		
1778	5.62	m	Benzene ring overtone	
1730	5.78	vs	C═N stretching	
1665	6.01	vs	C═N stretching or NH_2 bending	
1618	6.18	s	NH_2 scissoring deformation	Amines RNH_2
1540	6.49	s	Side chain asymmetric CN stretching	
1500	6.49	s	Benzene ring	
1453	6.88	s	In-plane C—H bending	
1416	7.06	w	In-plane C—H bending	
1389	7.20	w	CH or NH bending	
1336	7.49	w	—[c]	
1195	8.37	w	NH_2 rocking	
1170	8.55	w		
1091	9.17	w	C—C stretching	
1043	9.59	w	—[c]	
985	10.15	m	$—CH═CH_2$	
918	10.89	w	—[c]	
788	12.69	w	C═N torsion	
767	13.04	w	C—H bending deformation	Aromatic C—H
686	14.58	vw	Substituted benzene	
637	15.70	w	HCNC bending	
593	16.86	w	HNCN bending	
549 sh	18.21 sh	m	—[c]	
529	18.90	m	—[c]	

[a]Analysis is based on Bellamy (38), Szymanski (39), Pasto and Johnson (40), and Colthup (41).
[b]Intensity code: s = strong, m = medium, w. = weak, sh = shoulder.
[c]Unclassified.

persion relation analysis. This relationship is given by

$$[5] \qquad k(\omega) = \frac{-2\sqrt{R_N(\omega)}\sin\phi(\omega)}{1 + R_N(\omega) - 2\sqrt{R_N(\omega)}\cos\phi(\omega)}$$

where $R_N(\omega)$ is the normal-incidence reflectance at energy $\hbar\omega$ and $\phi(\omega)$, the phase change upon reflection at photon energy $\hbar\omega$, is given by

$$[6] \qquad \phi(\omega) = \frac{\omega}{\pi} P \int_0^\infty \frac{\ln R_N(\omega')}{(\omega')^2 - \omega^2} d\omega'$$

where P stands for the Cauchy principle value (42).

Normal-incidence reflectance values from 0.05 to 0.24 μm, where the reflectance was too low to measure directly, were extrapolated from the reflectance measured at non-normal angles of incidence. R_N was calculated in the 0.4–2.0 μm region using Fresnel's equation

$$[7] \qquad R_N = \frac{(n-1)^2 + k^2}{(n+1)^2 + k^2}$$

with the n and k values determined from ellipsometric and transmission measurements, respectively. For the 0.24–0.4 μm region, we calculated R_N by assuming that the real part of the index of refraction n equals 1.65 ± 0.02 for the entire region. The k values were determined from transmission measurements. For $\lambda > 0.4$ μm, we assumed a constant reflectance equal to the value at 0.4 μm since the reflectance in this low-energy region will not influence the values of k calculated in the K–K analysis in the 0.05–0.24 μm region. For the high-energy extrapolation ($\lambda < 0.05$ μm), we used the exponential form $R(E) = a \exp(-b)$ where the constants a and b were determined by requiring that the k values obtained in the K–K analysis agree with those determined earlier from transmission measurements in the region 0.19–0.24 μm.

The values of k obtained from this analysis are plotted in Fig. 5 and tabulated in Table 3. The k values are estimated to be accurate to ±20%. A detailed plot of k that clearly shows the 2.2 μm overtone band is shown for the wavelength range 1.5–5 μm (Fig. 6).

4.4. Kramers–Krönig analysis of n

A program based on the Kramers–Krönig relation between n

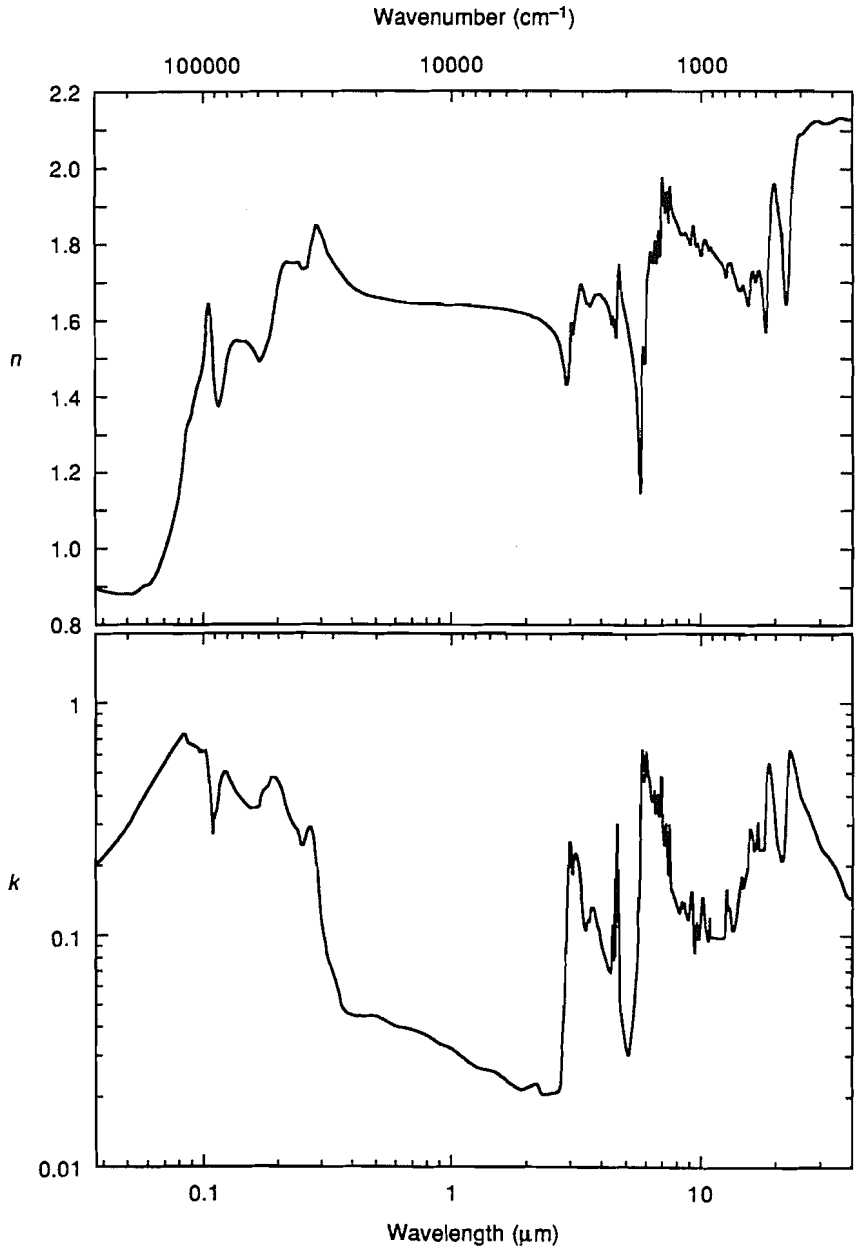

FIG. 5. Real (n) and imaginary (k) values of the complex refractive index as a function of wavelength of films prepared by thermal evaporation and redeposition under high vacuum of poly-HCN from du Pont Co.

and k (43) gave us n over the entire range of the measurements from the k values obtained above between 0.05 and 40 μm. The values of n were obtained from the following integral over the photon energy E

$$[8] \qquad n(E) - 1 = \frac{2}{\pi} P \int_0^\infty \frac{E'k(E')}{(E')^2 - E^2} \, dE'$$

The low-energy integration in eq. [8] was truncated at 100 μm, since the contribution to the integral from above 100 μm has no significant effect on the n values in the region of interest. A linear interpolation was chosen between $k = 0.144$ at $\lambda = 40$ μm and $k = 0.001$ at 100 μm. For the high-energy integration, the k values were extrapolated for $\lambda < 0.05$ μm using a power law $k = k(E_u)E^{-2}$, where $k(E_u)$ was the measured value of the imaginary part of the refractive index at 0.05 μm (24.8 eV), and E is in electron volts. The exponent −2 comes for the theoretical behavior of the imaginary part of the refractive index at high energies (42, 44). The high-energy cutoff for the integration was chosen to make the calculated values of n agree with the measured values in the 0.4–2.0 μm region. The values of n obtained from the Abeles (45) method from 0.4 to 0.625 μm agreed well with the values of n obtained using ellipsometry. The Abeles method is a variation of the Brewster angle method in which n is determined from scans of angular reflectance of thin films on thick substrates. The values of n from the K–K analysis agreed well with the values of n in the region from 0.05 to 0.24 μm determined by multi-angle reflectance measurements. The complete n spectrum from 0.05 to 40 μm is shown in Fig. 5. The n values

TABLE 3. Real (n) and imaginary (k) parts of the complex refractive index of thermally evaporated poly-HCN

λ (μm)	n	k	λ (μm)	n	k	λ (μm)	n	k
0.0373	0.896	0.200	0.194	1.634	0.477	2.233	1.605	0.0222
0.0401	0.890	0.218	0.205	1.718	0.432	2.251	1.604	0.0217
0.0432	0.885	0.239	0.216	1.752	0.352	2.276	1.602	0.0211
0.0475	0.882	0.273	0.227	1.751	0.307	2.300	1.600	0.0207
0.0494	0.883	0.289	0.240	1.752	0.280	2.349	1.595	0.0205
0.0502	0.884	0.296	0.248	1.740	0.245	2.398	1.591	0.0206
0.0506	0.883	0.300	0.250	1.735	0.244	2.448	1.586	0.0206
0.0510	0.882	0.304	0.252	1.733	0.245	2.500	1.579	0.0207
0.0514	0.881	0.309	0.253	1.733	0.244	2.541	1.574	0.0208
0.0523	0.882	0.319	0.258	1.735	0.264	2.583	1.567	0.0208
0.0560	0.894	0.367	0.260	1.737	0.272	2.623	1.560	0.0209
0.0576	0.900	0.387	0.262	1.738	0.278	2.656	1.552	0.0210
0.0593	0.905	0.408	0.264	1.742	0.286	2.685	1.544	0.0212
0.0602	0.905	0.420	0.266	1.754	0.286	2.703	1.538	0.0214
0.0610	0.906	0.430	0.268	1.769	0.292	2.715	1.534	0.0217
0.0616	0.908	0.438	0.270	1.782	0.291	2.730	1.528	0.0221
0.0629	0.916	0.454	0.272	1.795	0.292	2.740	1.522	0.0224
0.0677	0.959	0.517	0.274	1.804	0.282	2.778	1.502	0.0308
0.0750	1.054	0.616	0.276	1.813	0.273	2.831	1.475	0.0497
0.0805	1.145	0.690	0.278	1.821	0.263	2.857	1.452	0.0647
0.0827	1.198	0.720	0.280	1.829	0.247	2.897	1.433	0.113
0.0838	1.238	0.730	0.286	1.849	0.200	2.941	1.446	0.193
0.0849	1.279	0.725	0.290	1.846	0.165	2.963	1.477	0.242
0.0854	1.296	0.718	0.300	1.826	0.114	2.970	1.493	0.250
0.0866	1.322	0.683	0.305	1.814	0.102	2.985	1.528	0.251
0.0873	1.328	0.670	0.310	1.798	0.0925	2.995	1.548	0.250
0.0891	1.343	0.663	0.314	1.787	0.0847	3.008	1.575	0.242
0.0904	1.359	0.658	0.320	1.774	0.0775	3.030	1.593	0.202
0.0925	1.389	0.650	0.326	1.764	0.0733	3.040	1.589	0.190
0.0954	1.429	0.630	0.330	1.758	0.0701	3.050	1.582	0.186
0.0969	1.442	0.610	0.336	1.750	0.0662	3.060	1.574	0.185
0.0984	1.458	0.620	0.340	1.745	0.0639	3.068	1.567	0.185
0.100	1.483	0.610	0.344	1.740	0.0606	3.086	1.566	0.211
0.102	1.544	0.620	0.350	1.733	0.0569	3.100	1.579	0.217
0.103	1.581	0.600	0.356	1.726	0.0531	3.137	1.608	0.225
0.104	1.620	0.552	0.360	1.722	0.0498	3.160	1.625	0.221
0.105	1.635	0.501	0.366	1.716	0.0480	3.180	1.639	0.217
0.106	1.643	0.459	0.373	1.708	0.0468	3.200	1.651	0.212
0.108	1.607	0.349	0.380	1.702	0.0460	3.236	1.674	0.199
0.109	1.534	0.274	0.400	1.688	0.0450	3.297	1.693	0.154
0.111	1.443	0.327	0.500	1.659	0.0443	3.333	1.688	0.131
0.113	1.396	0.348	0.600	1.650	0.0402	3.400	1.669	0.110
0.115	1.377	0.406	0.700	1.645	0.0388	3.448	1.653	0.106
0.117	1.383	0.449	0.800	1.643	0.0366	3.483	1.645	0.113
0.119	1.404	0.480	0.900	1.642	0.0337	3.505	1.645	0.117
0.122	1.451	0.502	1.000	1.640	0.0322	3.522	1.645	0.117
0.124	1.483	0.500	1.100	1.639	0.0298	3.552	1.641	0.115
0.129	1.529	0.457	1.200	1.637	0.0278	3.571	1.638	0.118
0.133	1.543	0.428	1.300	1.635	0.0265	3.600	1.640	0.130
0.138	1.546	0.400	1.400	1.633	0.0261	3.664	1.652	0.132
0.149	1.543	0.362	1.500	1.632	0.0255	3.704	1.660	0.130
0.155	1.533	0.352	1.600	1.630	0.0243	3.780	1.668	0.119
0.163	1.511	0.352	1.700	1.627	0.0230	3.846	1.668	0.109
0.168	1.495	0.360	1.800	1.624	0.0221	3.899	1.669	0.105
0.170	1.493	0.390	1.900	1.620	0.0214	3.950	1.668	0.0950
0.175	1.508	0.421	2.000	1.617	0.0218	3.999	1.663	0.0892
0.182	1.539	0.437	2.100	1.612	0.0223	4.167	1.647	0.0763
0.188	1.578	0.477	2.200	1.606	0.0228	4.200	1.642	0.0740

TABLE 3. (*concluded*)

λ (μm)	*n*	*k*	λ (μm)	*n*	*k*	λ (μm)	*n*	*k*
4.300	1.622	0.0700	6.630	1.752	0.378	10.965	1.791	0.100
4.348	1.600	0.0694	6.650	1.766	0.399	11.169	1.780	0.0982
4.366	1.592	0.0827	6.667	1.783	0.405	11.500	1.769	0.0980
4.396	1.601	0.111	6.700	1.825	0.400	12.275	1.741	0.0978
4.428	1.613	0.0981	6.738	1.835	0.342	12.398	1.732	0.0984
4.468	1.584	0.0796	6.750	1.823	0.330	12.500	1.718	0.103
4.492	1.587	0.144	6.780	1.791	0.329	12.651	1.717	0.145
4.507	1.583	0.176	6.812	1.769	0.363	12.710	1.728	0.158
4.529	1.573	0.0862	6.850	1.788	0.438	12.781	1.741	0.150
4.558	1.555	0.185	6.887	1.870	0.480	12.903	1.748	0.131
4.589	1.637	0.288	6.965	1.975	0.340	13.072	1.748	0.132
4.598	1.655	0.154	6.993	1.968	0.301	13.189	1.751	0.122
4.651	1.720	0.191	7.042	1.937	0.262	13.333	1.740	0.108
4.696	1.746	0.0830	7.143	1.891	0.247	13.793	1.702	0.114
4.717	1.725	0.0487	7.160	1.885	0.252	14.388	1.678	0.161
4.762	1.682	0.0454	7.194	1.898	0.299	14.577	1.688	0.180
4.800	1.662	0.0430	7.250	1.937	0.259	14.706	1.691	0.164
5.000	1.603	0.0321	7.330	1.908	0.186	15.152	1.664	0.180
5.128	1.563	0.0305	7.353	1.886	0.185	15.385	1.642	0.200
5.263	1.516	0.0387	7.370	1.865	0.185	15.625	1.660	0.281
5.405	1.455	0.0511	7.380	1.857	0.191	16.000	1.723	0.270
5.556	1.344	0.0813	7.440	1.901	0.300	16.260	1.723	0.233
5.627	1.261	0.147	7.469	1.945	0.245	16.500	1.702	0.240
5.650	1.211	0.146	7.500	1.949	0.185	16.754	1.709	0.275
5.687	1.147	0.257	7.514	1.947	0.175	16.949	1.727	0.296
5.770	1.316	0.619	7.547	1.924	0.160	17.000	1.730	0.250
5.780	1.370	0.625	7.600	1.901	0.157	17.219	1.725	0.234
5.790	1.425	0.622	7.847	1.867	0.143	17.699	1.668	0.235
5.821	1.527	0.537	8.051	1.850	0.132	17.900	1.614	0.237
5.848	1.529	0.465	8.197	1.834	0.126	18.232	1.574	0.405
5.870	1.509	0.460	8.265	1.827	0.131	18.500	1.666	0.530
5.876	1.505	0.460	8.368	1.827	0.140	18.868	1.834	0.533
5.904	1.501	0.465	8.434	1.829	0.135	19.000	1.876	0.500
5.935	1.489	0.480	8.475	1.826	0.132	19.679	1.959	0.337
5.961	1.489	0.527	8.547	1.826	0.139	20.000	1.937	0.274
6.000	1.567	0.612	8.610	1.830	0.135	20.500	1.876	0.230
6.010	1.599	0.614	8.750	1.823	0.122	21.277	1.750	0.215
6.020	1.627	0.612	8.969	1.803	0.122	21.500	1.703	0.230
6.048	1.693	0.575	9.050	1.799	0.140	21.751	1.655	0.294
6.078	1.720	0.514	9.100	1.806	0.150	22.139	1.652	0.452
6.098	1.722	0.490	9.174	1.826	0.155	22.600	1.760	0.600
6.107	1.723	0.487	9.200	1.833	0.153	22.727	1.804	0.623
6.138	1.725	0.483	9.322	1.847	0.113	22.900	1.866	0.615
6.173	1.748	0.477	9.400	1.832	0.0900	24.310	2.075	0.460
6.199	1.765	0.462	9.434	1.821	0.0844	25.000	2.091	0.396
6.230	1.776	0.434	9.500	1.802	0.0900	26.000	2.098	0.360
6.262	1.779	0.406	9.537	1.795	0.0967	28.177	2.123	0.288
6.289	1.773	0.390	9.615	1.796	0.113	30.000	2.123	0.240
6.293	1.772	0.389	9.686	1.801	0.111	31.790	2.120	0.222
6.369	1.755	0.378	9.762	1.798	0.101	34.000	2.128	0.200
6.391	1.752	0.381	9.852	1.785	0.0968	35.423	2.133	0.183
6.424	1.757	0.395	9.998	1.771	0.121	38.000	2.131	0.150
6.457	1.779	0.414	10.080	1.776	0.138	40.000	2.132	0.144
6.485	1.804	0.409	10.152	1.789	0.146			
6.500	1.809	0.352	10.332	1.810	0.126			
6.525	1.806	0.339	10.526	1.804	0.104			
6.579	1.771	0.338	10.823	1.785	0.100			
6.600	1.759	0.340	10.893	1.788	0.120			

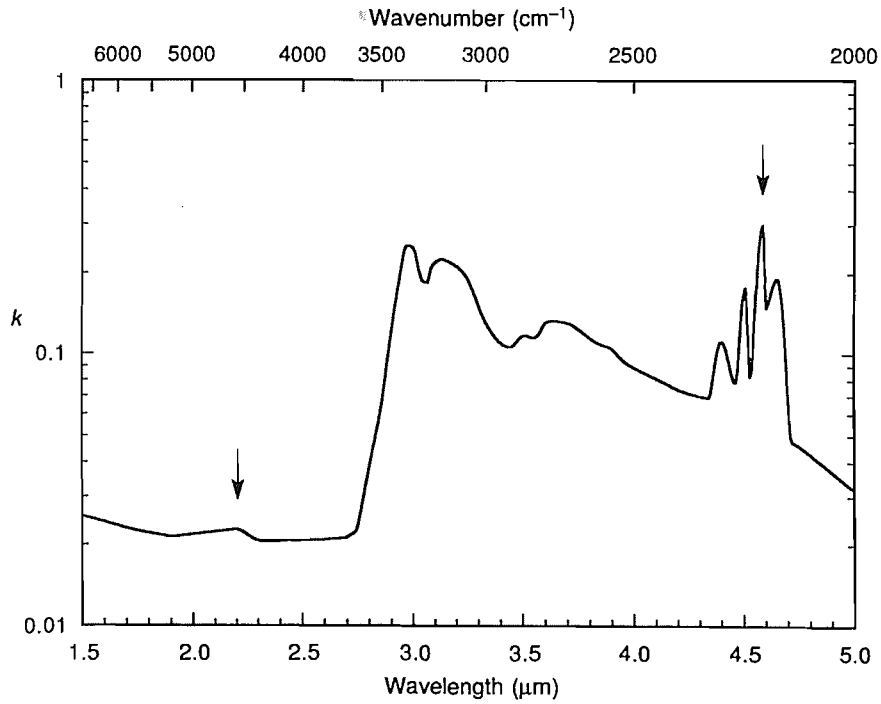

FIG. 6. The 2.2 μm overtone band of the C≡N stretching fundamental vibration at 4.5 μm in evaporated poly-HCN. Both features are marked by arrows.

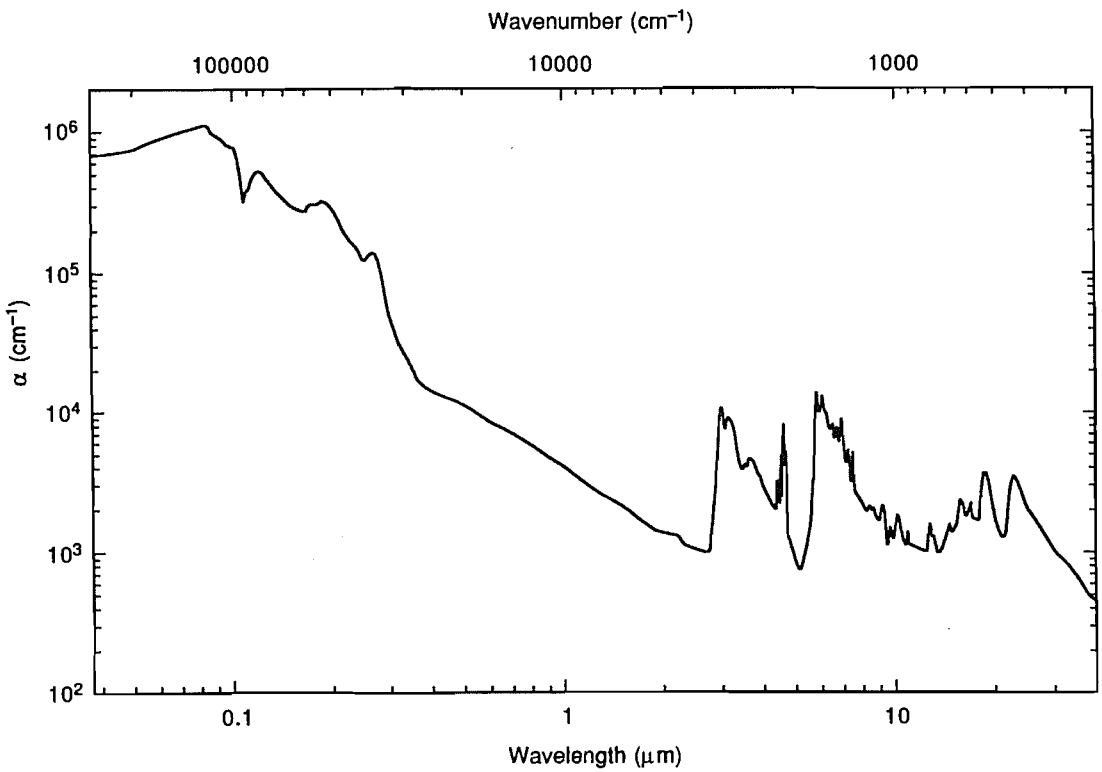

FIG. 7. Absorption coefficient (α) versus wavelength for evaporated and redeposited poly-HCN.

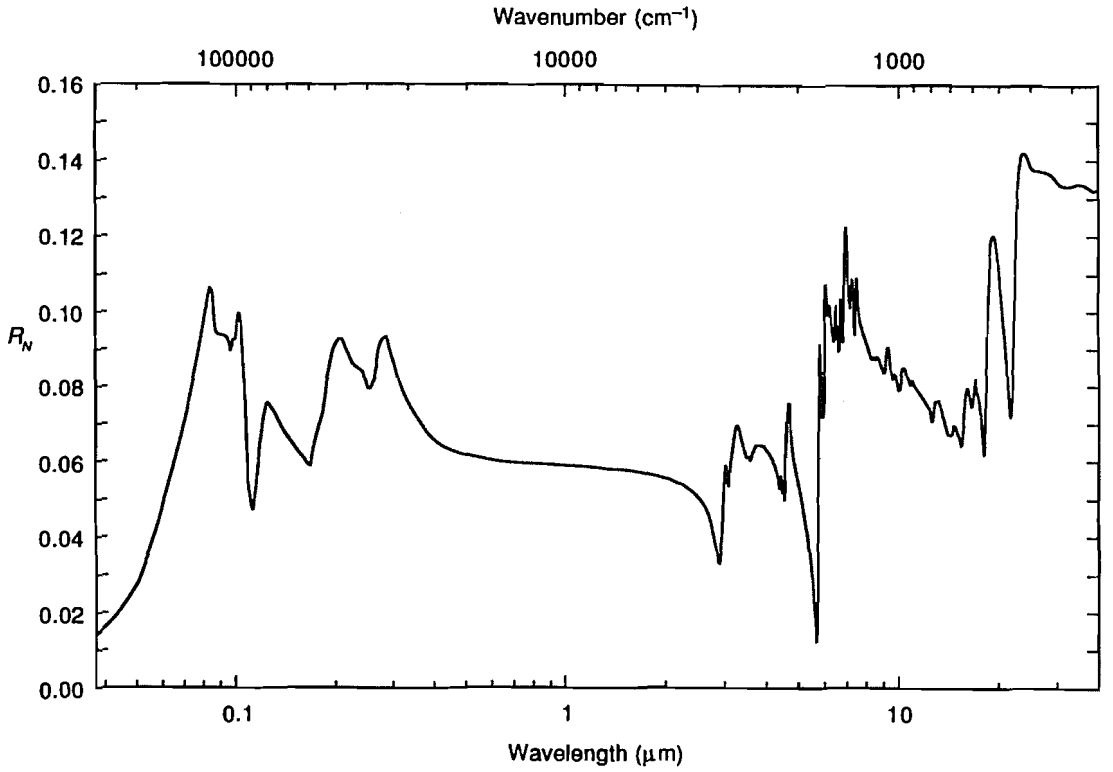

FIG. 8. Normal-incidence reflectance versus wavelength of evaporated and redeposited poly-HCN films.

are tabulated in Table 3 and are accurate to ±0.01 in absolute value and to ±0.002 on a relative scale.

4.5. Absorption coefficient, normal-incidence reflectance, dielectric function, and optical energy-loss function $Im(-1/\epsilon)$

The absorption coefficient α as a function of wavelength is shown in Figure 7. The normal-incidence reflectance R_N calculated from eq. [7] for a specular surface of poly-HCN is shown in Fig. 8. Dielectric constants $\epsilon_1 = n^2 - k^2$ and $\epsilon_2 = 2nk$ and the optical energy-loss function $\text{Im}(-1/\epsilon) = \epsilon_2/(\epsilon_1^2 + \epsilon_2^2)$ as a function of incident photon energy are shown in Fig. 9.

5. Comparison with the polymers of Bar-Nun et al. and Podolak et al.

Figure 10 shows the comparison of the imaginary part of the refractive index (k) of the evaporated and redeposited poly-HCN films determined in our investigation with the values calculated from the absorption coefficient ($-\log I/I_0$ per μm film thickness) of "poly-HCN" produced by Bar-Nun et al. (46) and Podolak et al. (47) from the photolysis of 5% HCN in CH_4 or argon. These authors identify their film as poly-HCN. Bar-Nun et al. (46) compare the absorption coefficients of their photochemically produced "poly-HCN" film with their photochemically produced polymers of C_2H_2 and C_2H_4, after correcting for the loss of light due to scattering. We assume that this correction also includes the loss of light due to reflection from the substrate and film. Thus, k is calculated for their photo-produced polymer (46) by substituting $-\log I/I_0$ values in the equation, $k = -0.183\lambda \log I/I_0\ \mu m^{-1}$, where λ is the wavelength in μm. We find poor agreement between our data and those of Bar-Nun et al. (46) and Podolak et al. (47), especially in the ultraviolet. For example, our k value at 0.21 μm is 3.96×10^{-1}, which is about an order of magnitude higher than the Bar-Nun et al. and Podolak et al. value of 2.5×10^{-2}. These authors have not displayed the infrared spectra of their putative poly-HCN so we cannot compare with the infrared spectra of other investigators.

Direct photolysis of HCN in the gas phase at 1850 Å yields $(CN)_2$, H_2, CH_4, NH_3, N_2H_4, C_2H_6, and CH_3NH_2 along with some undefined polymeric material (48). Becker and Hong (49) find similar products in their photolysis of HCN gas at 1850 Å except for H_2 and C_2H_6. They believe that H_2 is present but are unable to confirm this because of instrumental limitations. No "poly-HCN" is indicated by Mizutani et al. (48) or Becker and Hong (49) in their photolytic products. Mizutani et al. (48), in their study of the photochemical reaction of HCN and its polymeric products, refer to such polymers as "HCN polymers" only for convenience, since neither the composition nor the structures of the components of these materials are determined. Mizutani et al. caution that the degree of polymerization for some of the compounds may be sufficiently small that it may not be proper to call them polymers in the strict sense. Mizutani et al. (50) exhibit the infrared spectra of the brown polymer produced by the photochemical reaction of hydrogen cyanide in gas phase at 1849 Å; this may be what Bar-Nun et al. (46) would have obtained for their polymer. On comparing this spectrum with our unheated poly-HCN and vacuum-evaporated film of poly-HCN (Fig. 11), we find, as expected, spectral differences, although they are perhaps no more than the spectral differences among the several varieties of poly-HCN (Figs. 1, 2, 4). $(CN)_2$ is a major photolytic product of HCN and readily produces $(CN)_2$ ethanedinitrile homopolymers $(CN)_n$, also known as paracyanogen,

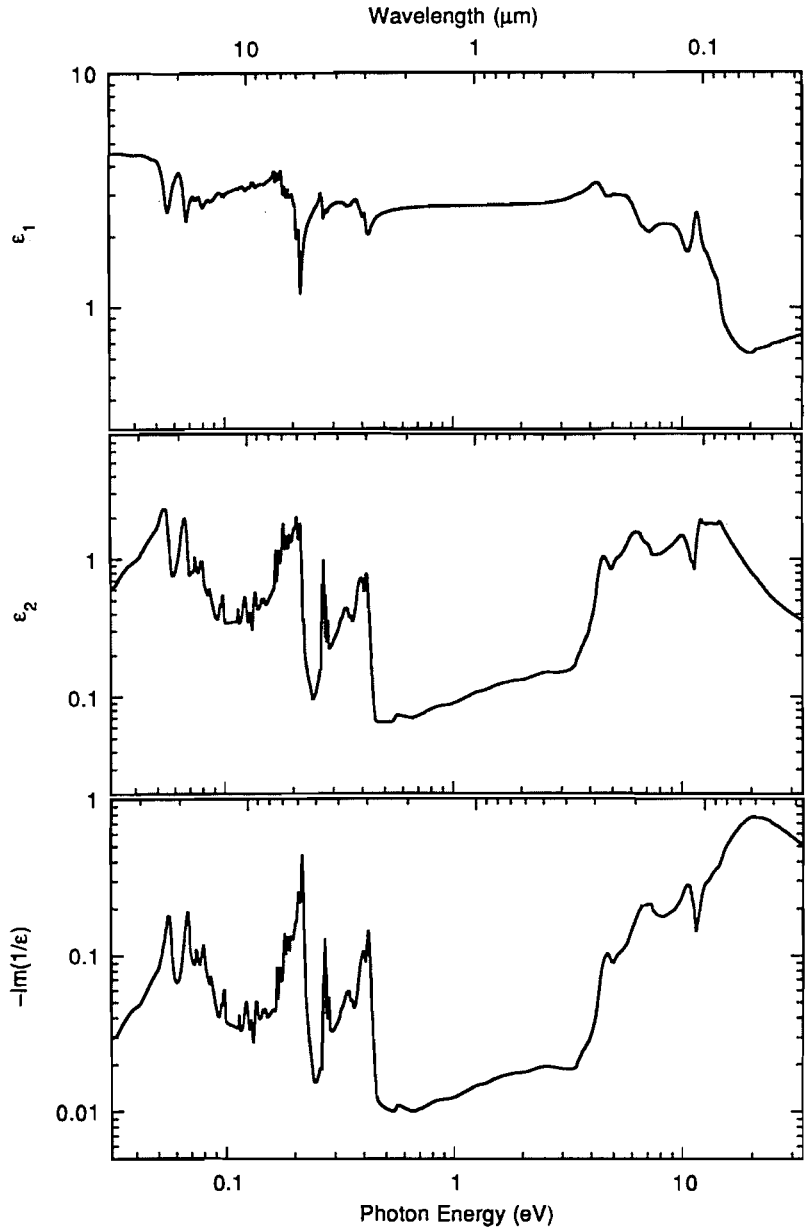

FIG. 9. Dielectric constants, ϵ_1 and ϵ_2, and energy loss function, $\mathrm{Im}(-1/\epsilon)$, of evaporated and redeposited poly-HCN as a function of photon energy.

on heating to above 400°C. It may be that Bar-Nun et al. and Podolak et al. have produced $(CN)_n$ polymer, possibly along with a Titan tholin-like material. This is further substantiated by the results of Hogness and Ts'ai (51) who found that C_2N_2 gas upon ultraviolet absorption between 2145 and 2240 Å dissociates either into two normal CN radicals or one normal and one excited CN radical, which combine with C_2N_2 producing $(CN)_3$. Thus the quantum efficiency for the photochemical reaction $(CN)_2 \rightarrow$ paracyanogen $[(CN)_n]$ is 3 moles per einstein.

Photons at 1847 Å employed by Bar-Nun et al. (46) and Podolak et al. (47) from a Hg-lamp photolysis of 5% HCN in CH_4 or argon have an energy of 6.7 eV. The approximate dissociation energy of the H—CN bond is 5.64 eV (52). Even if all the remaining 1.07 eV is partitioned to the H atom as kinetic energy, it is still insufficient to dissociate CH_4 (the bond dissociation energy for H—CH_3 is 4.42 eV.) However, it may be possible that the CN radical could attack CH_4, triggering reactions leading to Titan tholin-like material. A comparison with the imaginary part of the refractive index (k) of Titan tholin (12) is also shown in Fig. 10. The data of Bar-Nun et al. and Podolak et al., as expected, do not fit the optical constants data for Titan tholin either. Bar-Nun et al. and Podolak et al. also state that their $-\log I/I_0$ values are essentially the same whether the polymer is produced by photolyzing 5% HCN in CH_4 or Ar. This clearly indicates that CH_4 does not participate in the production of their polymer, eliminating the possibility of a Titan tholin-like material being produced.

Bar-Nun et al. and Podolak et al. did not measure the density of their polymer, but instead assumed a value of 1.18 g cm^{-3}, that of polyacrylonitrile (53). We measured the density of the du Pont poly-HCN employed in our measurement of the opti-

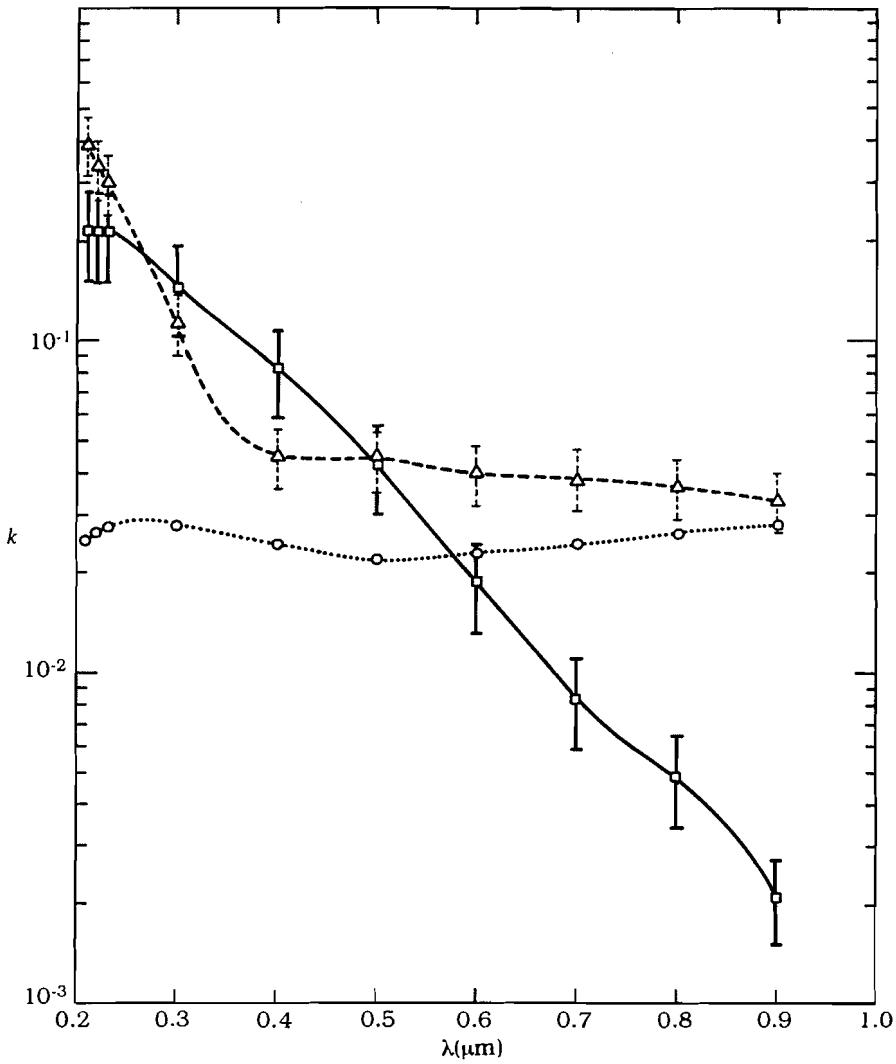

FIG. 10. Comparison of the imaginary part of the refractive index (k) of poly-HCN determined in this investigation (△) with the values calculated from the $-\log I/I_0$ per μm thick film of poly-HCN produced from the photolysis of 5% HCN in CH_4 or argon by Bar-Nun et al. (46); Podolak et al. (47) (○). Imaginary part of the refractive index (k) of Titan tholin (12) is also shown (□).

cal constants by helium pycnometry and found a value of 1.620 ± 0.004 g cm^{-3} for the du Pont poly-HCN. With this higher density, a thinner film thickness, which produces higher k values, is obtained. However, these new k values still do not help produce a match with the k values reported here. We conclude that the polymer produced by Bar-Nun et al. and Podolak et al. is not poly-HCN. It could be mainly paracyanogen with a Titan tholin-like material and a minor component of poly-HCN.

6. Comparison with other bodies in the solar system

The specular reflectance of smooth surfaces of poly-HCN in the visible part of the spectrum (Fig. 8) is about 6%. This is in the range of estimates for cometary nuclei and other dark surfaces in the outer solar system. But many other plausible organic materials have similar reflectances, for example, organic residues produced by irradiation of mixtures of hydrocarbon and water ices (19).

As an example of the application of these optical constant results to claims of abundant poly-HCN in the outer solar system, consider the haze of Saturn's large satellite Titan. Matthews (1, 54) proposes that this is due to poly-HCN and generated from HCN in the Titanian atmosphere. In Fig. 12, we plot in crosshatching the values of k from 0.3 to 0.9 μm for the Titan haze (55) deduced from groundbased data of the geometric albedo (56–58) and from 16.67 to 40 μm from Voyager spacecraft observations (59). The deduced values for $k(\lambda)$ are derived from standard models of atmospheric structure and aerosol distribution. The reduced data apply from the near ultraviolet to the middle infrared, with, unfortunately, no observations available between about 1.5 and about 10 μm, where possibly diagnostic chemical functional groups lie. If spectral features were detectable in the near- to middle-infrared, other diagnostic distinctions might be made (for example, note the difference in ratios of the 3 μm C—H absorption features and the 4.5 μm C≡N features in poly-HCN compared with Titan tholin.) Plotted in the same figure are the results of the present paper for poly-HCN and the optical constants obtained in the laboratory for Titan tholin, the organic solid produced by irradiating simulated Titanian atmospheres (12, 60). Estimated uncertainties in the model-dependent values of k for the Titan haze are about ±40% (61), while those for the laboratory observations are estimated to be about ±20% for poly-HCN and ±30% for Titan tholin. Titan tholin fits the Titan observations

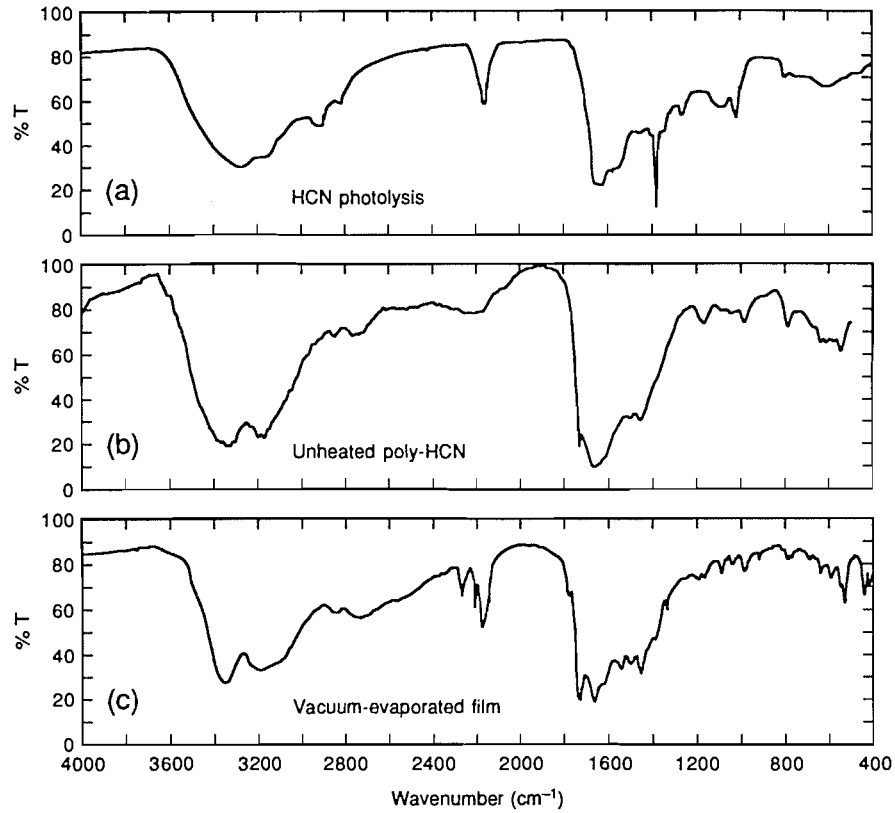

FIG. 11. The infrared spectra of (*a*) brown polymer produced by the photochemical reaction of hydrogen cyanide in gas phase at 1849 Å (50) is compared with (*b*) unheated poly-HCN and (*c*) vacuum evaporated film of poly-HCN.

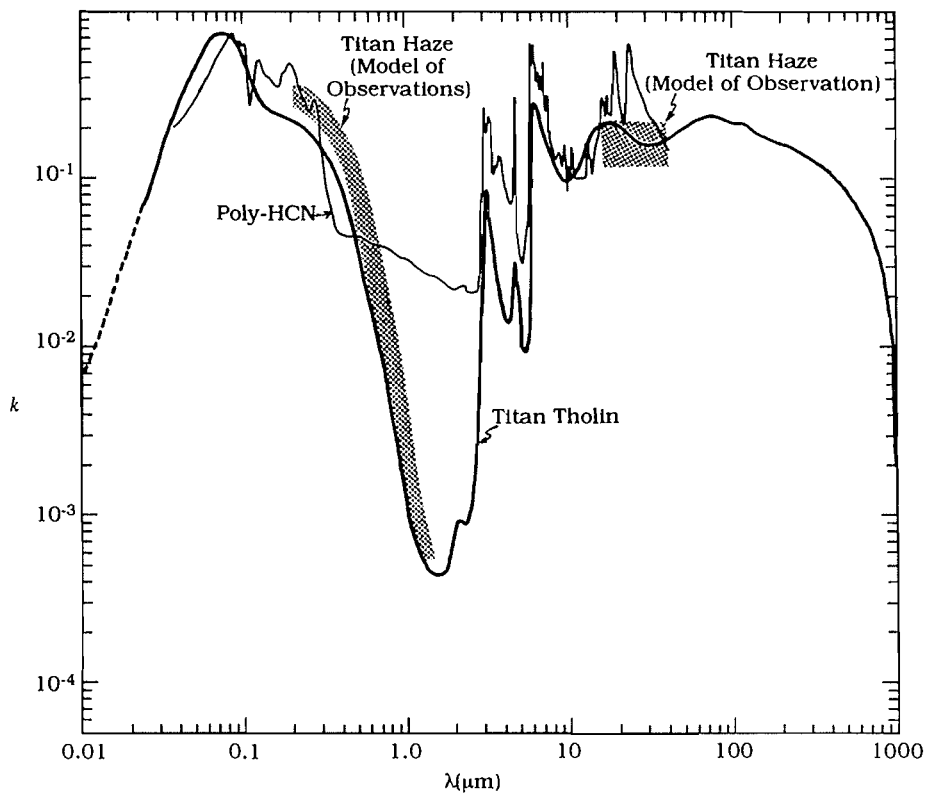

FIG. 12. Comparison of the imaginary part, *k*, of the complex refractive index from 0.3 to 0.9 μm of the organic haze of Titan (55), derived from groundbased data of the geometric albedo (56–58) and from 16.67 to 40 μm (59) after normalizing *k* at 40 μm, with *k* for poly-HCN (this paper), and for the organic residue (Titan tholin) obtained from plasma discharge through a 9:1 N_2/CH_4 mixture (60, 12). Probable errors of the groundbased data are shown by the stippling from 0.2 to 1.0 μm, *k* from 16.67 to 40 μm is normalized to Titan tholin at 40 μm. Probable errors for the laboratory measurements are about ±20% for poly-HCN and ±30% for Titan tholin.

within the probable errors (60), and no other proposed material does. It is apparent that, in the visible and near-infrared, the fit is far better for Titan tholin than for poly-HCN. Titan tholin is much redder in the visible than poly-HCN, and poly-HCN displays a sharp discontinuity (absorption edge) at about 0.35 μm, which neither the Titan haze nor Titan tholin display. In the long visible and near-infrared, poly-HCN exhibits one to two orders of magnitude larger values of k than does Titan or Titan tholin. Poly-HCN can therefore be at best a minor constituent of the Titan haze.

The volatile component of Titan tholin, when examined by sequential and nonsequential pyrolytic GC–MS, reveals over 100 products, including aliphatic hydrocarbons, nitriles, polycyclic aromatic hydrocarbons, amines, pyroles, pyrazines, pyridines, pyrimidines, and, perhaps, the purine adenine (15, 17). Independent evidence for the presence of PAHs has now been found (62). A number of these compounds are not present in poly-HCN and would not be expected to be released on volatilization of poly-HCN. In addition, of course, it makes intuitive sense that the organic solid generated by irradiation of simulated Titanian atmospheres, experiments that successfully and quantitatively reproduce the gas-phase organics in Titan's atmosphere (63), should be the best candidate for the organic haze of Titan (60).

Pesce-Rodriguez et al. (64) suggest that the similarity between "HCN polymers" and the Murchison meteorite is "striking", at least in the middle infrared. However, a comparison of the optical constants of poly-HCN, reported here, and those of an organic residue from the Murchison carbonaceous chondrite (18) reveals major discrepancies. Meteoritic organics are not poly-HCN.

As model optical constants of other hazes and surfaces in the outer solar system become available, they also can be compared with laboratory optical constants of poly-HCN, tholins, and other materials, as done here for Titan, and the claims for poly-HCN assessed on a case-by-case basis. Much simpler comparisons of laboratory with planetary spectra may also be useful, but may not be nearly as definitive. The exclusion of poly-HCN as the principal constituent of the Titan haze does not exclude its presence elsewhere. It might, for example, be that poly-HCN is too neutrally colored in the visible to explain reddish clouds and surfaces, but might be a useful model for much blacker surfaces. However, other, perhaps more likely, materials — such as some PAHs or elemental carbon (or tholins produced from CH_4) — may prove more successful. Because of its low albedo and explosive polymerization, poly-HCN is a reasonable candidate for the dark lag deposit of cometary nuclei. Our measured values of the optical constants may find use in modelling of the cometary dust.

We have recently used Hapke scattering theory and a linear superposition of the optical constants of a number of materials in an attempt to explain the observed spectrum of 5145 Pholus, a very red asteroid or comet on an eccentric orbit with aphelion beyond Uranus (65). All good fits seem to require ~10% poly-HCN, or some other material with similar strong absorption in the near-infrared.

7. Acknowledgements

This research was supported by NASA grant NAGW 3273, "Studies of Satellite and Planetary Atmospheres", NASA Planetology Grant NAGW 1870, the Kenneth T. and Eileen L. Norris Foundation, and by the U.S. Department of Energy contract DE-AC05-84OR 21400 with Martin Marietta Energy Systems, Inc. We thank C.N. Matthews for stimulating this study and for supplying poly-HCN for our preliminary spectral studies, R. Geyer and L. Pesce of du Pont for bulk samples of poly-HCN employed in the measurement of the optical constants, and Chris McKay for his interest and advice in this project.

1. C.N. Matthews. Origins Life, **21**, 421 (1992).
2. C.N. Matthews and R. Ludicky. Proc. ESLAB Symp. 20th, Exploration of Halley's Comet. Eur. Space Agency [Spec. Publ.] ESA SP-250, 273 (1986).
3. C.N. Matthews and R. Ludicky. Solid State NMR Polym. [Proc. Annu. Chem. Conf. North Am. Solid State NMR Polym.], 3rd, 1988. *Edited by* L.J. Mathais. Plenum, New York. 1991. p. 331.
4. M. Allen, J.P. Pinto, and Y.L. Yung. Astrophys. J. **242**, L125 (1980).
5. D.P. Cruikshank, L.J. Allamandola, W.K. Hartmann, D.J. Tholen, R.H. Brown, C.N. Matthews, and J.F. Bell. Icarus, **94**, 345 (1991).
6. C.N. Matthews. The search for extraterrestrial life: recent developments. *Edited by* M.D. Papagiannis. 1985. p. 151.
7. C.N. Matthews and R.E. Moser. Proc. Natl. Acad. Sci. U.S.A. **56**, 1087 (1966).
8. C.N. Matthews and R.E. Moser. Nature, **215**, 1230 (1967).
9. B.N. Khare and C. Sagan. Icarus, **20**, 311 (1973).
10. C. Sagan and B.N. Khare. Nature, **277**, 102 (1979).
11. C. Sagan, B.N. Khare, and J.S. Lewis. Saturn. *Edited by* T. Gehrels and M.S. Matthews. University of Arizona Press, Tucson. 1984. p. 788.
12. B.N. Khare, C. Sagan, E.T. Arakawa, F. Suits, T.A. Callcott, and M.W. Williams. Icarus, **60**, 127 (1984).
13. G.D. McDonald, B.N. Khare, W.R. Thompson, and C. Sagan. Icarus, **94**, 354 (1991).
14. B.N. Khare, C. Sagan, J.E. Zumberge, D.S. Sklarew, and B. Nagy. Icarus, **48**, 290 (1981).
15. B.N. Khare, C. Sagan, W.R. Thompson, E.T. Arakawa, F. Suits, T.A. Callcott, M.W. Williams, S. Shrader, H. Ogino, T.O. Willingham, and B. Nagy. Adv. Space Res. **4**, 59 (1985).
16. B.N. Khare, C. Sagan, H. Ogino, B. Nagy, C. Er, K.H. Schram, and E.T. Arakawa. Icarus, **68**, 176 (1986).
17. P. Ehrenfreund, J.J. Boon, J. Commandeur, C. Sagan, W.R. Thompson, and B.N. Khare. Adv. Space Res. In press.
18. B.N. Khare, W.R. Thompson, C. Sagan, E.T. Arakawa, C. Meisse, and I. Gilmour. Proc. Int. Conf. Lab. Res. Planetary Atmospheres, 1st, NASA CP-3077, 340 (1990).
19. B.N. Khare, W.R. Thompson, L. Cheng, C. Chyba, C. Sagan, E.T. Arakawa, C. Meisse, and P.S. Tuminello. Icarus, **103**, 290 (1993).
20. A.F. Lunin, L.A. Pakhomov, V.A. Vinokurov, V.F. Novikov, V.N. Barybin, V.R. Mkrtychan, and A.V. Burobin. Khim. Vys. Energ. **12**, 380 (1978).
21. S.L. Miller. J. Am. Chem. Soc. **77**, 2351 (1955).
22. C. Sagan and S.L. Miller. Astron. J. **65**, 499 (1960).
23. K. Ziegler. Hydrogen cyanide (anhydrous) organic synthesis. Vol. I. *Edited by* Henry Gilman. John Wiley & Sons, Inc., New York. 1932. p. 307.
24. W.R. Jenks. Kirk–Othmer concise encyclopedia of chemical technology. Wiley–Interscience Publications, New York. 1985. p. 334.
25. T. Völker. Angew. Chem. **69**, 728 (1957).
26. T. Völker. Angew. Chem. **72**, 379 (1960).
27. R.A. Evans, P. Lorenčak, T. Ha, and C. Wentrup. J. Am. Chem. Soc. **113** 7261 (1991).
28. R.A. Evans, S.M. Lacombe, M.J. Simon, G. Pfister-Guillouzo, and C. Wentrup. J. Phys. Chem. **96**, 4801 (1992).
29. J.P. Ferris and W.J. Hagan, Jr. Tetrahedron, **40**, 1093 (1984).

30. R.A. Sanchez, J.P. Ferris, and L.E. Orgel. J. Mol. Biol. **30**, 223 (1967).
31. J.P. Ferris, D.B. Donner, and W. Lotz. J. Am. Chem. Soc. **94**, 6968 (1972).
32. J.P. Ferris and E.H. Edelson. J. Org. Chem. **43**, 3989 (1978).
33. J.P. Ferris. Science, **203**, 1135 (1979).
34. C.N. Matthews and R. Ludicky. Adv. Space Res. **12**, 21 (1992).
35. T.W. Rettig, S.C. Tegler, D.J. Pasto, and M.J. Mumma. Astrophys. J. **398**, 293 (1992).
36. F. Woeller and C. Ponnamperuma. Icarus, **10**, 386 (1969).
37. B.N. Khare and C. Sagan. Science, **189**, 722 (1975).
38. L.J. Bellamy. The infrared spectra of complex molecules. John Wiley & Sons, New York. 1975.
39. H.A. Szymanski. Infrared band handbook. Plenum, New York. 1963.
40. D.J. Pasto and C.R. Johnson. Organic structure determination. Prentice-Hall, Inc., Englewood Cliffs, N.J. 1969.
41. N.B. Colthup. J. Opt. Soc. Am. **40**, 397 (1950).
42. M.W. Williams, E.T. Arakawa, and T. Inagaki. *In* Handbook on synchrotron radiation. Vol. 4. *Edited by* S. Ebashi, M. Koch, and E. Rubenstein. Elsevier Science Publishers, New York. 1991.
43. T. Inagaki, L.C. Emerson, E.T. Arakawa, and M.W. Williams. Phys. Rev. B, **13**, 2305 (1976).
44. M.W. Williams, R.N. Hamm, E.T. Arakawa, L.R. Painter, and R.D. Birkhoff. Int. J. Radiat. Phys. Chem. **7**, 95 (1975).
45. F. Abeles. J. Phys. Radium, **11**, 310 (1950).
46. A. Bar-Nun, I. Kleinfeld, and E. Ganor. J. Geophys. Res. **93**, 8383 (1988).
47. M. Podolak, N. Noy, and A. Bar-Nun. Icarus, **40**, 193 (1979).
48. H. Mizutani, H. Mikuni, M. Takahasi, and N. Noda. Origins Life, **6**, 513 (1975).
49. R.S. Becker and J.H. Hong. J. Phys. Chem. **87**, 163 (1983).
50. H. Mizutani, H. Mikuni, and M. Takahasi. Chem. Lett. 573 (1972).
51. T.R. Hogness and L. Ts'ai. J. Am. Chem. Soc. **54**, 123 (1932).
52. J.G. Calvert and J.N. Pitts, Jr. Photochemistry. John Wiley & Sons, Inc., New York. 1966. p. 826.
53. J. Brandrup and E.H. Immergut. Polymer handbook. Interscience, New York. 1966.
54. C.N. Matthews. Origins Life, **12**, 281 (1982).
55. C.P. McKay, J.B. Pollack, and R. Courtin. Icarus, **80**, 23 (1989).
56. J.S. Neff, D.C. Humm, J.T. Bergstrahl, A.L. Cochran, W.D. Cochran, E.S. Barker, and R.G. Tull. Icarus, **60**, 221 (1984).
57. J.S. Neff, T.A. Ellis, J. Apt, and J.T. Bergstrahl. Icarus, **62**, 425 (1985).
58. U. Fink and H.P. Larson. Astrophys. J. **233**, 1021 (1979).
59. R.E. Samuelson and L.A. Mayo. Icarus, **91**, 207 (1991).
60. C. Sagan, W.R. Thompson, and B.N. Khare. Acc. Chem. Res. **25**, 286 (1992).
61. C.P. McKay and O.B. Toon. Proc. Symp. Titan. Eur. Space Agency, [Spec. Publ.] ESA SP 338, 185 (1992).
62. C. Sagan, B.N. Khare, W.R. Thompson, G.D. McDonald, M.R. Wing, J.L. Bada, T. Vo-Dinh, and E.T. Arakawa. Astrophys. J. **414**, 399 (1993).
63. W.R. Thompson, T.J. Henry, J.M. Schwartz, B.N. Khare, and C. Sagan. Icarus, **90**, 57 (1991).
64. R.A. Pesce-Rodriguez, S.A. Liebman, and C.N. Matthews. Int. Conf. Origins Life, Barcelona, 10th, July 4–9, 1993.
65. P.D. Wilson, C. Sagan, and W.R. Thompson. Icarus. In press.